Optical response of nonlinear multilayer structures: Bilayers and superlattices

Wei Chen and D. L. Mills
Department of Physics, University of California, Irvine, California 92717
(Received 30 March 1987)

We discuss the normal-incidence reflectivity and transmissivity of a multilayer structure which contains N films, each of which has a dielectric constant dependent on light intensity, through a term proportional to the local intensity. We show the method introduced in a previous paper for the isolated film [Wei Chen and D. L. Mills, Phys. Rev. B **35**, 524 (1987)] may be generalized to the present case, retaining the feature that a numerical solution may be achieved by means of a search for a single real number bounded between zero and unity. Explicit calculations for a bilayer show that such a structure exhibits bistability with nonreciprocal character: The threshold for the onset of bistability with light incident from the left may differ substantially from that with light incident from the right. We also apply the theory to finite superlattices. For frequencies close to the edge of a stop gap of the structure, for rather low power, we find the system may switch from a state where the transmissivity is unity to a state where it is exponentially small. Solitons play a key role as mediators of the switching in extended superlattices.

I. INTRODUCTION

The nonlinear optical response of matter has been studied theoretically and experimentally for a number of years. The presence of high-power laser sources raises questions about the nature of the response of materials well beyond the regime where a perturbation theoretic treatment is valid. One finds a variety of instabilities at such high power levels, one of which is bistability in which the material may switch from a state of low transmissivity to high, as laser power increases.

Phenomena such as bistability occur because the dielectric constant of the material depends on the amplitude or intensity of the electromagnetic wave. In materials with a center of inversion, symmetry forbids the appearance of terms linear in the field amplitude, so the lowest-order contributions are quadratic in this quantity. In the simplest picture, we may suppose the index of refraction depends on the intensity of the optical wave.

There is a considerable current literature devoted to another aspect of electromagnetic propagation in dielectric media, under conditions when nonlinear response is important. This is the theoretical analysis of surface polariton propagation, on the interface between a semiinfinite material with quadratic nonlinearities such as those just described, and a linear dielectric.[1,2] For such waves, of course, the fields vanish far from the interface. This condition, when exploited mathematically, leads to simplifications that allows the solution to the nonlinear problem to be expressed in terms of elementary functions, for a number of models of interest.

If there is a finite rate of energy transport normal to the interface between a linear and nonlinear medium, as is the case in the analysis of the reflection of light off a film or interface, it is no longer possible to obtain solutions in such a form even for the simplest models of the nonlinear response. This greatly complicates the rigorous analysis of bistability in dielectric films. For plane polarized light normally incident on the film, the general solution may be expressed in terms of the Jacobi elliptic functions.

A practical difficulty arises because the general solution involves four parameters whose value must be such that the relevant boundary conditions are satisfied, and these are buried within the Jacobi elliptic function in a nontrivial manner. A numerical search within the appropriate four-dimensional space is formidable. Through a series of identities derived from the boundary conditions, in a previous paper,[3] we were able to express three of the parameters in terms of a fourth, known to be bounded between zero and unity. The problem of calculating the transmissivity of the nonlinear film then becomes straightforward, from a numerical point of view.

This paper is devoted to the analysis of a multilayer structure which consists of N nonlinear films, of thickness $d_1, d_2, \ldots, d_N$. We address the problem of calculating the transmission of radiation through the structure, at normal incidence. Within each film, the general solution to the wave equation once again involves four parameters constrained by the boundary conditions, and so we have $4N$ in total for the whole structure. We show here how these may be interrelated through use of arguments similar to those used earlier,[3] so in the end we may achieve a solution once again by searching for a single parameter which lies between zero and unity.

We use this formalism to analyze bistability in a two layer structure, to find nonreciprocal behavior. The threshold for the onset of bistability as laser power is either increased or decreased is different when the laser beam strikes the structure incident from the left, compared to the values found with the beam incident from the right.

We have also studied the power dependence of the transmissivity of a superlattice structure which contains

a finite number of unit cells. The infinitely extended superlattice has stop gaps when described by linear response theory, and electromagnetic waves with frequency within such a stop gap have amplitude which decays exponentially as they propagate down the structure. Our calculations show that if a finite superlattice with nonlinear response is illuminated with radiation whose frequency lies within a stop gap, under suitable conditions the system may switch between a state where the transmissivity is unity, to a state of very low transmissivity, as the laser power is decreased. This switching occurs for rather low laser powers, as we shall see. The numerical calculations, supplemented by a recent approximate analytic treatment of the optical response of nonlinear superlattices,[4] establish that solitons excited by the incident electromagnetic wave play a central role in such systems. The reader should note that a brief description of the superlattice calculations has appeared elsewhere.[5] The present paper presents a full discussion of the formalism used in the earlier calculations, along with new results.

Before we proceed with our discussion, we note that Delyon *et al.*[6] have studied the nonlinear response of finite superlattices illuminated by radiation with frequency outside the stop gaps of linear response theory. They also find rich structure in the power dependence of the transmissivity, in such a spectral regime. Our studies combined with theirs show this to be a field with great potential for future experiments.

II. GENERAL DISCUSSION

We consider a plane-polarized electromagnetic wave which propagates parallel to the z direction; the surface of the multilayer structure will be normal to the z axis. The wave vector of the electromagnetic wave in vacuum is $k_0=\omega/c$, and if n is the index of refraction of a medium at low power, the wave vector in the medium is $k=n\omega/c$. The basic wave equation in the media of interest then has the form

$$\frac{d^2E}{dz^2}+k^2(1+\lambda\,|\,E\,|^2)E=0\ , \tag{2.1}$$

where λ is a nonlinear coefficient that may be either positive or negative. Each film in our multilayer structure is described by an equation such as Eq. (2.1), and the linear index of refraction and nonlinear coefficient may differ from film to film.

If E_0 is the magnitude of the incident electric field outside the structure, we measure field in units of E_0 everywhere by writing

$$E(z)=E_0\mathcal{E}(z)\exp[i\phi(z)]\ , \tag{2.2}$$

where substitution into Eq. (2.1) gives

$$\frac{d^2\mathcal{E}}{dz^2}-\mathcal{E}\left[\frac{d\phi}{dz}\right]^2+k^2(1+\tilde{\lambda}\mathcal{E}^2)\mathcal{E}=0 \tag{2.3a}$$

and

$$\frac{d\mathcal{E}}{dz}\frac{d\phi}{dz}+\frac{1}{2}\mathcal{E}\frac{d^2\phi}{dz^2}=0 \tag{2.3b}$$

with $\tilde{\lambda}=\lambda\,|\,E_0\,|^2$. The incident field may now be taken to have unit amplitude, and the intensity dependence of the response of the structure is explored by scaling the values of the various nonlinear coefficients $\tilde{\lambda}_m$, with $\tilde{\lambda}_m$ the nonlinear coefficient of the mth film.

One may integrate Eq. (2.3b) to give

$$\frac{d\phi}{dz}=\frac{W}{\mathcal{E}^2}\ , \tag{2.4}$$

where W is the rate of energy flow parallel to the z direction.[3] In the theory of nonlinear surface polaritons one has $W=0$. Notice upon substituting Eq. (2.4) into Eq. (2.3a) we have

$$\left[\frac{d\mathcal{E}}{dz}\right]^2+\frac{W^2}{\mathcal{E}^2}+k^2\mathcal{E}^2+\tfrac{1}{2}k^2\tilde{\lambda}\mathcal{E}^4=A\ , \tag{2.5}$$

with A a constant of integration. Let the material of interest terminate at $z=d$, and let $I(z)=\mathcal{E}^2(z)$. Then upon integrating Eq. (2.5), we have

$$\int_{I(d)}^{I(z)}dI\frac{1}{(AI-k^2I^2-\frac{1}{2}k^2\tilde{\lambda}I^3-W^2)^{1/2}}=\pm 2k(z-d)\ , \tag{2.6}$$

where either sign is allowed on the right-hand side. Also,

$$\phi(z)=\phi(d)+W\int_d^z dz'\frac{1}{I(z')}\ . \tag{2.7}$$

The general solution just outlined contains the four parameters W, A, $I(d)$, and $\phi(d)$ which are constrained by the relevant boundary conditions, as we shall see.

The relations just given apply within each film of our multilayer structure, with the various parameters replaced by values appropriate to the relevant film. If either $\tilde{\lambda}=0$, or as in the theory of surface polaritons $W=0$, the integral on the left-hand side of Eq. (2.6) may be evaluated in terms of elementary functions. In general, as we have seen,[3] the integral is expressed in terms of Jacobi elliptic functions. We consider first the linear case $\tilde{\lambda}=0$, then $\tilde{\lambda}>0$ and $\tilde{\lambda}<0$ separately.

A. The case $\tilde{\lambda}=0$

Upon integrating Eq. (2.6) we have

$$\sin^{-1}\left[\frac{2k^2I(z)-A}{(A^2-4k^2W^2)^{1/2}}\right]-\sin^{-1}\left[\frac{2k^2I(d)-A}{(A^2-4k^2W^2)^{1/2}}\right]=\pm 2k(z-d)\ , \tag{2.8}$$

which yields

$$I(z)=\frac{1}{2k^2}\left\{A+(A^2-4k^2W^2)^{1/2}\sin\left[\pm 2k(z-d)+\sin^{-1}\left[\frac{2k^2I(d)-A}{(A^2-4k^2W^2)^{1/2}}\right]\right]\right\} . \tag{2.9}$$

The boundary conditions between adjacent media require both $I(z)$ and its normal derivative to the continuous, as we shall see. We shall discuss the means of choosing the ambiguous sign below.

B. The case $\tilde{\lambda}>0$

Consider the roots of the polynomial which appears in the denominator of Eq. (2.6). If we let $I=I'-\frac{2}{3}\tilde{\lambda}$, then these roots are found from

$$(I')^3-pI'+q=0 , \tag{2.10}$$

where we have

$$p=\frac{4}{3\tilde{\lambda}^2}+\frac{2A}{k^2\tilde{\lambda}} \tag{2.11a}$$

and

$$q=\frac{16}{27\tilde{\lambda}^3}+\frac{4A}{3k^2\tilde{\lambda}^2}+\frac{2W^2}{k^2\tilde{\lambda}} . \tag{2.11b}$$

Obviously, for $\tilde{\lambda}>0$, p, and q are positive. It is known that there are three real and unequal roots if $27q^2<4p^3$, but there is one real root and two complex conjugate roots if $27q^2>4p^3$. We shall see soon that the optical intensity $I(z)$ is bounded inside the film. The only physically reliable solution requires the coefficients p and q to satisfy $27q^2<4p^3$ for any nonzero $\tilde{\lambda}$. We shall always be able to find a solution consistent with this constraint. If we define an angle θ such that

$$\cos(3\theta)=(27q^2/4p^3)^{1/2} ,$$

then we have three roots given by

$$I^{(n)}=-\frac{2}{3\tilde{\lambda}}-\left[\frac{4p}{3}\right]^{1/2}\cos\left[\theta+\frac{2\pi}{3}n\right] , \tag{2.12}$$

where $n=1$, 2, and 3. We refer to the roots as $I^{(1)}$, $I^{(2)}$, and $I^{(3)}$, and we shall always arrange the roots so that $I^{(1)}>I^{(2)}>I^{(3)}$.

The integral in Eq. (2.6) may then be written

$$\int_{I(d)}^{I(z)}dI\frac{1}{[(I^{(1)}-I)(I^{(2)}-I)(I^{(3)}-I)]^{1/2}}=\pm(2\tilde{\lambda})^{1/2}k(z-d) . \tag{2.13}$$

The integral on the left-hand side can be expressed in terms of the inverse of a Jacobi elliptic function. We suppose $I^{(2)}<I(z)<I^{(1)}$, and then one has

$$\mathrm{cn}^{-1}\left[\frac{[I(z)-I^{(2)}]^{1/2}}{(I^{(1)}-I^{(2)})^{1/2}}\middle|\frac{I^{(1)}-I^{(2)}}{I^{(1)}-I^{(3)}}\right]-\mathrm{cn}^{-1}\left[\frac{[I(d)-I^{(2)}]^{1/2}}{(I^{(1)}-I^{(2)})^{1/2}}\middle|\frac{I^{(1)}-I^{(2)}}{I^{(1)}-I^{(3)}}\right]=\pm[\tfrac{1}{2}\tilde{\lambda}(I^{(1)}-I^{(3)})]^{1/2}k(d-z) . \tag{2.14}$$

This may be rearranged to read

$$I(z)=I^{(2)}+(I^{(1)}-I^{(2)})\mathrm{cn}\left[\psi(z)\middle|\frac{I^{(1)}-I^{(2)}}{I^{(1)}-I^{(3)}}\right] , \tag{2.15a}$$

where

$$\psi(z)=\pm[\tfrac{1}{2}\tilde{\lambda}(I^{(1)}-I^{(2)})]^{1/2}k(d-z)+\mathrm{cn}^{-1}\left[\frac{[I(d)-I^{(2)}]^{1/2}}{(I^{(1)}-I^{(2)})^{1/2}}\middle|\frac{I^{(1)}-I^{(2)}}{I^{(1)}-I^{(3)}}\right] . \tag{2.15b}$$

Once again, we comment below on the choice of sign on the right-hand side of Eq. (2.15a).

C. The case $\tilde{\lambda}<0$

We now let $I=I'+\frac{2}{3}|\tilde{\lambda}|$ to convert the denominator of Eq. (2.6) to the form in Eq. (2.10), with

$$p=p'=\frac{4}{3|\tilde{\lambda}|^2}-\frac{2A}{k^2|\tilde{\lambda}|} \tag{2.16a}$$

and

$$q=q'=\frac{16}{27|\tilde{\lambda}|^3}-\frac{4A}{3k^2|\tilde{\lambda}|^2}+\frac{2W^2}{k^2|\tilde{\lambda}|} . \tag{2.16b}$$

When the condition $27(q')^2<4(p')^3$ is satisfied, we again have three real roots of the cubic, given by

$$I^{(n)}=\frac{2}{3|\tilde{\lambda}|}+\left[\frac{4p'}{3}\right]^{1/2}\cos\left[\theta-\frac{2\pi}{3}(n-1)\right] , \tag{2.17}$$

with

$$\cos(3\theta)=[27(q')^2/4(p')^3]^{1/2} ,$$

and we always arrange the roots so that $I^{(1)}>I^{(2)}>I^{(3)}$. We then have

$$\int_{I(d)}^{I(z)} dI \frac{1}{[(I-I^{(1)})(I-I^{(2)})(I-I^{(3)})]^{1/2}} = \pm 2(|\tilde{\lambda}|^{1/2})k(z-d) . \tag{2.18}$$

We shall find the calculated intensities lie in the range $I^{(3)}<I(z)<I^{(2)}$ and then once more the integral on the left-hand side of Eq. (2.18) may be expressed in terms of Jacobi elliptic functions. We have now

$$\mathrm{cn}^{-}\left[\left[\frac{(I^{(1)}-I^{(2)})[I(z)-I^{(3)}]}{(I^{(2)}-I^{(3)})[I^{(1)}-I(z)]}\right]^{1/2}\left|\frac{I^{(2)}-I^{(3)}}{I^{(1)}-I^{(3)}}\right.\right]-\mathrm{cn}^{-1}\left[\left[\frac{(I^{(1)}-I^{(2)})[I(d)-I^{(3)}]}{(I^{(2)}-I^{(3)})[I^{(1)}-I(d)]}\right]^{1/2}\left|\frac{I^{(2)}-I^{(3)}}{I^{(1)}-I^{(3)}}\right.\right]$$
$$=\mp(I^{(1)}-I^{(3)})^{1/2}\left[\frac{|\tilde{\lambda}|}{2}\right]^{1/2}k(z-d) . \tag{2.19}$$

Inverting this relation gives, with

$$\psi(z)=\mp(I^{(1)}-I^{(3)})^{1/2}\left[\frac{|\tilde{\lambda}|}{2}\right]^{1/2}k(z-d)+\mathrm{cn}^{-1}\left[\left[\frac{(I^{(1)}-I^{(2)})[I(d)-I^{(3)}]^{1/2}}{(I^{(2)}-I^{(3)})[I^{(1)}-I(d)]}\right]^{1/2}\left|\frac{I^{(2)}-I^{(3)}}{I^{(1)}-I^{(3)}}\right.\right] , \tag{2.20}$$

$$I(z)=\frac{N(z)}{D(z)} \tag{2.21}$$

where

$$N(z)=I^{(3)}(I^{(1)}-I^{(2)})+I^{(1)}(I^{(2)}-I^{(3)})\mathrm{cn}^2\left[\psi(z)\left|\frac{I^{(2)}-I^{(3)}}{I^{(1)}-I^{(3)}}\right.\right] \tag{2.22a}$$

and

$$D(z)=(I^{(1)}-I^{(2)})+(I^{(2)}-I^{(3)})\mathrm{cn}^2\left[\psi(z)\left|\frac{I^{(2)}-I^{(3)}}{I^{(1)}-I^{(3)}}\right.\right] . \tag{2.22b}$$

D. The boundary conditions

In the preceding subsections, we have outlined the general solution of the nonlinear wave equation in the medium. The solution requires four parameters be determined. One is $I(d)$, the second is W, there is the integration constant A which appears in Eq. (2.5), and finally $\phi(d)$ in Eq. (2.7). Of course, the number of free parameters is the same as for the linear dielectric, where the most general solution of the wave equation consists of a superposition of two plane waves, one running from left to right and one from right to left. Each plane wave has a complex amplitude which consists of a modulus and a phase.

In the multilayer structure, we have four parameters in each film, so if there are N films in the multilayer structure, the general solution within the medium contains $4N$ parameters. If we consider the reflectivity of the multilayer medium (at normal incidence), then we encounter $4N+4$ parameters, since an amplitude and phase are required for both the reflected and the transmitted wave.

In our earlier paper,[3] where transmission through a single film was considered, we found that a sequence of identities can be derived from the boundary conditions which interrelate enough parameters that a solution may be achieved for searching for only one. This is W, a positive real number bounded by the condition the transmissivity be less than unity always. We now turn to this question once again, for the multilayer structure.

We consider a multilayer structure which consists of N layers, each designated with the index $m=1,2,3,\ldots,N$. The boundary conditions are that both the electric field and its first derivative must be continuous at $z=0$, where the incident wave encounters the structure, and $z=d_m$, the boundary between the mth and $(m+1)$st film.

With R the complex amplitude of the reflected wave, at $z=0$ the boundary conditions read (recall $k_0=\omega/c$), with $\mathcal{E}_m(z)$ and $\phi_m(z)$ the amplitude and phase of the electric field in the mth film

$$1+R=\mathcal{E}_1(0)e^{i\phi_1(0)} \tag{2.23a}$$

and

$$1-R=\frac{1}{ik_0}\left[\frac{d\mathcal{E}_1}{dz}\right]_{z=0}e^{i\phi_1(0)}+\frac{1}{k_0}e^{i\phi_1(0)}\mathcal{E}_1(0)\left[\frac{d\phi_1}{dz}\right]_{z=0}. \tag{2.23b}$$

At $z=d_N$, where we match the solution inside the structure to the transmitted wave, we have

$$Te^{ik_0d_N}=\mathcal{E}_N(d_N)e^{i\phi_N(d_N)} \tag{2.24a}$$

and

$$Te^{ik_0d_N}=\frac{1}{ik_0}\left[\frac{d\mathcal{E}_N}{dz}\right]_{z=d_N}e^{i\phi_N(d_N)}+\frac{e^{i\phi_N(d_N)}}{k_0}\mathcal{E}_N(d_N)\left[\frac{d\phi_N}{dz}\right]_{z=d_N}. \tag{2.24b}$$

At the boundary between two films in the structure, we have

$$\mathcal{E}_m(d_m)e^{i\phi_m(d_m)}=\mathcal{E}_{m+1}(d_m)e^{i\phi_{m+1}(d_m)} \tag{2.25a}$$

and

$$\left[\frac{d\mathcal{E}_m}{dz}\right]_{z=d_m}e^{i\phi_m(d_m)}+i\left[\frac{d\phi_m}{dz}\right]_{z=d_m}\mathcal{E}_m(d_m)e^{i\phi_m(d_m)}=\left[\frac{d\mathcal{E}_{m+1}}{dz}\right]_{z=d_m}e^{i\phi_{m+1}(d_m)}+i\left[\frac{d\phi_{m+1}}{dz}\right]_{z=d_m}\mathcal{E}_{m+1}(d_m)e^{i\phi_{m+1}(d_m)}. \tag{2.25b}$$

As in our previous paper, we may combine Eq. (2.23a) and Eq. (2.23b) to give the constraint

$$4k_0^2=\left[\left[\frac{d\mathcal{E}_1}{dz}\right]_{z=0}\right]^2+\mathcal{E}_1^2(0)\left[k_0+\left[\frac{d\phi_1}{dz}\right]_{z=0}\right]^2, \tag{2.26}$$

while from Eqs. (2.24) we have

$$\left[\frac{d\mathcal{E}_N}{dz}\right]_{z=d_N}=0 \tag{2.27a}$$

and

$$\frac{1}{k_0}\left[\frac{d\phi_N}{dz}\right]_{z=d_N}=1. \tag{2.27b}$$

We now turn to constraints one may obtain from Eqs. (2.25). Upon separating the real and imaginary parts of Eqs. (2.25a) and (2.25b), squaring these, and adding, we have

$$\mathcal{E}_m^2(d_m)=\mathcal{E}_{m+1}^2(d_m). \tag{2.28}$$

We may divide Eq. (2.24b) into Eq. (2.24a), and separate the real and imaginary parts to find

$$\left[\frac{1}{\mathcal{E}_m}\frac{d\mathcal{E}_m}{dz}\right]_{z=d_m}=\left[\frac{1}{\mathcal{E}_{m+1}}\frac{d\mathcal{E}_{m+1}}{dz}\right]_{z=d_m} \tag{2.29a}$$

and also

$$\left[\frac{d\phi_m}{dz}\right]_{z=d_m}=\left[\frac{d\phi_{m+1}}{dz}\right]_{z=d_m}. \tag{2.29b}$$

Since $\mathcal{E}_m(z)$ is always positive, by definition, Eq. (2.28a) also implies $\mathcal{E}_m(d_m)=\mathcal{E}_{m+1}(d_m)$, a condition which when combined with Eq. (2.29a) gives

$$\left[\frac{dI_m}{dz}\right]_{z=d_m}=\left[\frac{dI_{m+1}}{dz}\right]_{z=d_m}. \tag{2.30}$$

Upon combining Eqs. (2.28a) with Eq. (2.29b) and Eq. (2.4), we find

$$W_m=W_{m+1}=W, \tag{2.31}$$

so the solution in each film of the structure is characterized by the same value of W, a requirement in fact which must be satisfied to insure energy conservation. However, from the point of view of a numerical search for a solution, Eq. (2.31) eliminates $(N-1)$ parameters from the initial set of $4N+4$.

The relations given above also lead to the constraint

$$A_m=A_{m+1}+k_0^2(n_m^2-n_{m+1}^2)I_{m+1}(d_m)+\tfrac{1}{2}k_0^2(n_m^2\tilde{\lambda}_m-n_{m+1}^2\tilde{\lambda}_{m+1})I_{m+1}^2(d_m). \tag{2.32}$$

Within the outermost film, we have the special relations in Eqs. (2.27a) and (2.27b) which apply at $z=d_N$. This allows us to obtain a relation between W and A_N:

$$A_N=k_0(1+n_N^2)W+\tfrac{1}{2}n_N^2\tilde{\lambda}_NW^2. \tag{2.33}$$

A solution to the multilayer problem now proceeds as follows. In our units, W is a real number bounded between zero and k_0. We begin by guessing a value of W. This gives us $I_N(d_n)$ through the relation $W=k_0I(d_N)$, and from Eq. (2.33) we may find A_N. We may then calculate $I_N(z)$ throughout the Nth film using Eq. (2.21). (The sign ambiguities must be resolved before this can be done uniquely. We comment on this issue below). From $I_N(z)$, we may calculate $I_N(d_{N-1})$, which must equal $I_{N-1}(d_{N-1})$ by virtue of Eq. (2.30). We know that $W_{N-1}=W_N=W$, and we may use Eq. (2.32) to find A_{N-1}, with this information. Now we know enough to calculate $I_{N-1}(z)$ everywhere within the $(N-1)$st film. We may continue this procedure to calculate $I_m(z)$ throughout each film in the multilayer structure. This may be done without requiring input information on the phase $\phi(z)$, notice. If desired, phase information may be obtained from Eq. (2.7), once $I(z)$ is known.

Thus, given a guess for the single real number W, we can construct the solution everywhere in the multilayer structure. We need a criterion from which we may decide when we have chosen a correct value of this parameter. We do this as in our earlier paper. We may add Eq. (2.23a) from Eq. (2.23b) to find

$$2e^{-i\phi(0)}=\mathcal{E}_1(0)+\frac{1}{ik_0}\left[\frac{d\mathcal{E}_1}{dz}\right]_{z=0}+\frac{1}{k_0}\frac{W}{\mathcal{E}_1(0)} \tag{2.34}$$

which when separated into real and imaginary parts yields

$$2\cos[\phi(0)]=\mathcal{E}_1(0)+\frac{1}{k_0}\frac{W}{\mathcal{E}_1(0)} \tag{2.35a}$$

and

$$2\sin[\phi(0)]=\frac{1}{k_0}\left[\frac{d\mathcal{E}_1}{dz}\right]_{z=0}. \tag{2.35b}$$

We may square both sides of Eq. (2.35a), add them to Eq. (2.35b) after squaring each side in a similar manner, then use Eq. (2.5) to eliminate $[(d\mathcal{E}_1/dz)_{z=0}]^2$. When written in terms of $I_1(z)$, we find

$$\tfrac{1}{2}n_1^2\tilde{\lambda}_1 I_1^2(0)+(n_1^2-1)I_1(0)+4-2\frac{W}{k_0}-\frac{A}{k_0^2}=0\ . \tag{2.36}$$

If this equation is satisfied after a value of W is selected, then we have a solution to the multilayer problem.

We may scan the parameter W through the range $0<W<k_0$, and search for the particular values which yield a solution consistent with the boundary conditions. The problem of calculating the transmissivity or reflectivity of the multilayer structure thus reduces to a search for the allowed values of W.

There remains the question of the choice of sign in the arguments of the Jacobi elliptic functions which appear in Eq. (2.15a) and Eqs. (2.18). These are determined by noting that at each interface, the derivatives dI/dz are continuous [Eq. (2.30)]. Thus, one computes $(dI_{m+1}/dz)_{z=d_m}$, and notes that the choice of sign in $I_m(z)$ must be such that the derivatives match at the boundary. This will be the case only for one choice of sign.

There are instances where the slope vanishes at the interface, so this criterion is inapplicable. This is always the case at the outer interface, as we see from Eq. (2.27a). One then uses the following identity:

$$\left[\frac{d^2I_m}{dz^2}\right]_{z=d_m}=\left[\frac{d^2I_{m+1}}{dz^2}\right]_{z=d_m}+2(k_{m+1}^2-k_m^2)I_{m+1}(d_m)+2(k_{m+1}^2\tilde{\lambda}_{m+1}-k_m^2\tilde{\lambda}_m)I_{m+1}^2(d_m)\ . \tag{2.37}$$

At the interface between the outermost film and vacuum, since we have a plane wave in the vacuum, the second derivative on the right-hand side of Eq. (2.37) vanishes, and $\tilde{\lambda}_{m+1}$ may be set to zero. Satisfaction of the identity at the boundary then allows the ambiguous sign to be determined. We now turn to the results of our numerical studies of multilayer structures which incorporate films that exhibit a nonlinear optical response.

III. RESULTS AND DISCUSSION

In Fig. 1 we show the transmissivity of a bilayer in which the second of the two films is endowed with a nonlinear index of refraction; the first film is the film exposed to the incident radiation. In the linear theory, the value of the transmissivity is left unchanged if the bilayer is replaced by its mirror image, or if it is illuminated from the right instead of from the left. The dashed curves in Fig. 1, and the solid curve are calculated for the bilayer and its mirror image, for the case where one of the two films is endowed with a power-dependent index of refraction, modeled as in Sec. II. We see the transmissivity is now highly nonreciprocal. Such bilayers will thus have the property that in a given power range, they will exhibit bistability when illuminated from the left, but not from the right.

As discussed in a brief publication[5] and mentioned earlier, we also have applied the formalism to the study of power dependent transmission through superlattice structures with a finite length. We turn next to a more complete description of this sequence of calculations, and their implication.

Within the framework of linear theory, an infinitely extended superlattice provides an example of the classic Kronig-Penny model used to illustrate wave propagation in periodic structures.[7] The normal modes have the character of Bloch waves which propagate down the structure, and the associated dispersion relation possesses stop gaps at the Brillouin-zone boundaries. For the particular structure studied here, in the reduced

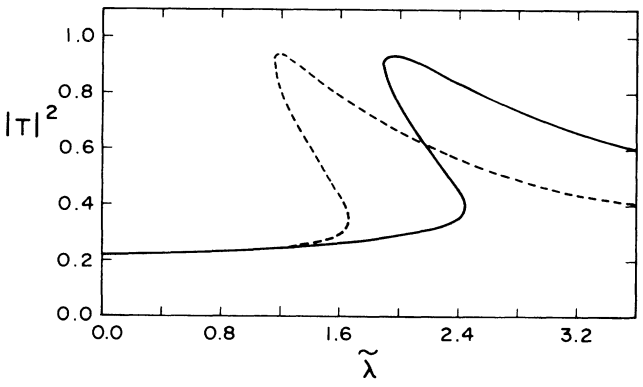

FIG. 1. The transmissivity as a function of power of two bilayers, one the mirror image of the other. The solid curve is a calculation of the transmissivity for $d_1=0.13\lambda_1$ and $d_2=0.2\lambda_2$, where $\lambda_{1,2}=\lambda_0/n_{1,2}$ and $n_1=6$, $n_2=4$, with λ_0 the vacuum wavelength of the incident radiation. Also, for the solid curve, $\tilde{\lambda}_1=\lambda$ and $\tilde{\lambda}_2=0$. The dashed curve is the calculation for the mirror image of the bilayer just described.

zone scheme, we show the two lowest branches in the dispersion relation in Fig. 2.

In Fig. 3 we show the transmissivity of a finite length of the model superlattice used to generate the dispersion curves in Fig. 2; the calculations are for a superlattice which contains twenty unit cells. The frequency lies in the stop gap of Fig. 2, just a bit above the lower band edge at $\omega=0.74\pi$. Film 1 is a linear dielectric film ($\lambda_1=0$), while film 2 has a nonlinear coefficient $\lambda_2<0$. The curve in Fig. 3 is identical to that displayed in Fig. 1(a) of Ref. 5, though we have chosen here to rearrange the material a bit.

At low powers, for frequencies within the stop gap, the transmissivity is very small, since the amplitude of the wave in the superlattice has an envelope which decays exponentially, in linear theory. For this example, at low power the transmissivity $|T|^2$ is in the 10^{-4} range. Thus, on the graph in Fig. 3, we cannot resolve its value from zero. As the power is increased, we see the folding back of $|T|^2$, plotted as a function of laser power, in a manner familiar from discussions of optical bistability. The transmissivity becomes a multivalued function of power (or $\tilde{\lambda}_2$) above $|\tilde{\lambda}_2|>0.0035$. The system will thus "switch" at rather low values of power.

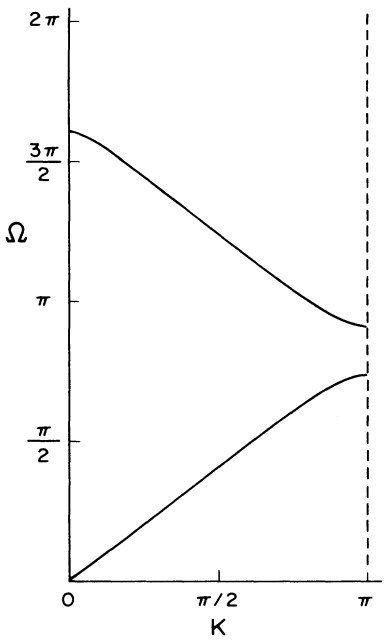

FIG. 2. The two lowest branches of the dispersion curve for electromagnetic wave propagation down the model superlattice studied in the present paper, in linear theory. The two films in each unit cell have equal thickness, $d_1=d_2$. A dimensionless measure of frequency is $\Omega=\omega n_1(d_1+d_2)/c$, with ω the actual frequency of the wave. A dimensionless measure of wave vector is $K=k(d_1+d_2)$, with k the actual wave vector. We have chosen $d_1=d_2=0.125\lambda_0$, where λ_0 is the vacuum wavelength of a photon with frequency $\pi c/(d_1+d_1)$. We choose $n_1=1.5$, and $n_2=2.12$, corresponding to dielectric constants $\epsilon_1=2.25$ and $\epsilon_2=4.50$.

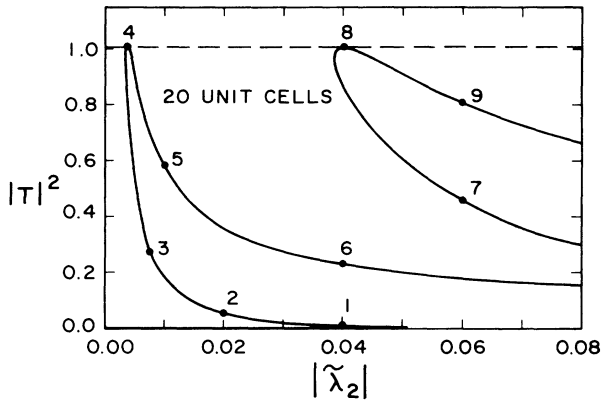

FIG. 3. For the superlattice described in Fig. 2, we plot the transmissivity $|T|^2$ as a function of power, for a finite superlattice with twenty unit cells. The frequency Ω, in units used in Fig. 2, is 0.75π, and lies in the stop gap, just above the bottom edge at 0.74π. Film 1 is a linear dielectric film ($\lambda_1=0$), while for film 2, λ_2 is negative.

So far as we can tell from our numerical work, the transmissivity at both point 4 and point 8, the peaks in the two distorted "resonance curves," assumes the value of unity. Thus, if the superlattice is illuminated with radiation of the appropriate power, and with frequency in the stop gap, it becomes quite transparent. We have carried out calculations for a number of frequencies near the lower gap edge, and superlattices of various length (see below) and with different choice of index of refraction, and we always find such behavior, though the power required to reach threshold varies from case to case. Near the lower gap edge, we find such behavior only when $\lambda_2<0$, and for frequencies near the upper gap edge, we must choose $\lambda_2>0$. We have not been able to integrate the equations accurately, for frequencies which are very far removed from either gap edge.[8] Thus, our attention here is necessarily confined to the near gap edge region.

Insight into the physical origin of the transmission

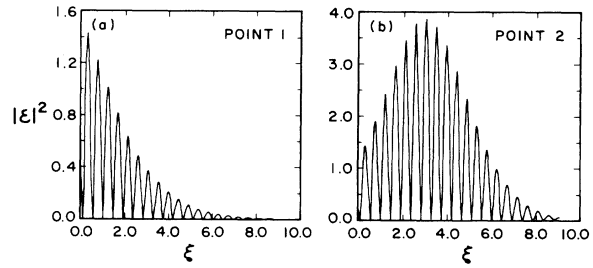

FIG. 4. The square of the electric field $|(z)|^2$ within the finite superlattice, at (a) point 1 and (b) point 2 in the curve in Fig. 3. The amplitude of the incident field is unity. The coordinate ξ is a dimensionless measure of length in the superlattice. Within film 1, length is measured in units of λ_0/n_1 and within film 2, length is measured units of λ_0/n_2. In these units, $d_1=0.1875$ and $d_2=0.2652$.

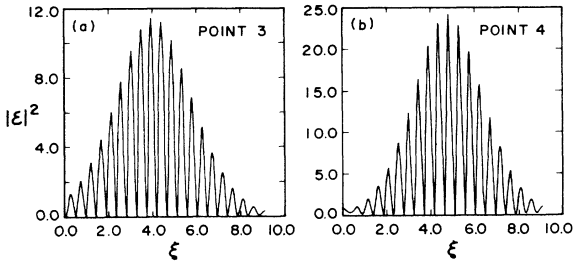

FIG. 5. The same as Fig. 4, but now the field intensity is calculated (a) at point 3 and (b) at point 4 of Fig. 3.

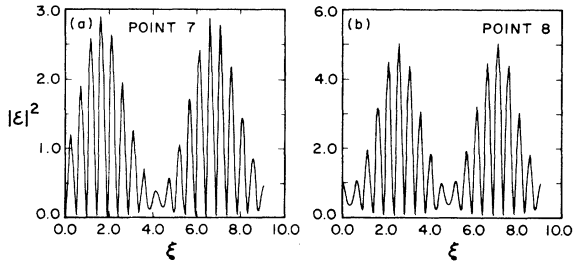

FIG. 7. The same as Fig. 4, but now the field is calculated at (a) point 7, and (b) point 8 of Fig. 3.

resonances displayed in Fig. 3 may be obtained by plotting the intensity of the field within the superlattice $|\mathcal{E}(z)|^2$ at various points on the curve of transmissivity versus power, given in Fig. 3. This is done for the nine points labeled in Fig. 3 as shown in Figs. 4–8.

Figure 4(a) shows the variation of $|\mathcal{E}(z)|^2$ at point 1 of Fig. 3, which lies on the reentrant portion of the transmissivity curve, above the lowest curve which coincides with the $|T|^2=0$ axis to within graphical accuracy. The envelope of $|\mathcal{E}(z)|^2$ decays monotonically, in a manner similar to one's expectations from linear theory, which provides a pure exponentially decaying envelope. As we move to point 2, the envelope initially *increases,* rather than decreases, a behavior that differs qualitatively from that provided by linear theory, when the periodic structure is illuminated by a frequency within a stop gap. This tendency is more pronounced and dramatic at point 3, as illustrated in Fig. 5.

Point 4 is the field distribution at resonance, so to speak, where the finite superlattice has become perfectly transparent to the radiation whose frequency lies within the stop gap. The envelope, to the eye, reminds one of the envelope of a sine-Gordon soliton. Indeed, we find the envelope is fitted rather nicely by the function $\cosh^{-2}(\alpha\xi)$, with an appropriate choice of α. This is the case, save near the two surfaces of the superlattice. At point 5 the soliton center has shifted to the right, it has shrunk a bit in width, and we see the "tail" of a second solitonlike structure entering the film from the left-hand side, which is the side illuminated by the incident photon.

For all these calculations, the amplitude of the incident field has been taken equal to unity. Notice as one progresses from point 2 to point 4, the maximum value of $|\mathcal{E}|^2$ in the structure increases quite dramatically, and then drops as one moves from point 4 to point 5.

In our earlier numerical work,[5] we demonstrated that for an infinitely extended superlattice, the nonlinear equations admit a soliton solution in the limit $W=0$. The field associated with such a soliton is displayed in Fig. 2 of Ref. 5. More recently, it has been possible to demonstrate by analytic methods that the phase $\phi(z)$ obeys a double sine-Gordon equation when $W=0$, and the soliton states may be described analytically,[4] in terms of elementary functions, at least in certain limits.

The previous paragraph refers to soliton solutions of the nonlinear equations in the limit of a superlattice of infinite spatial extent. If the superlattice is finite, and one sets up a soliton at time $t=0$, it will have a finite lifetime because it may radiate its energy into the vacuum on either side of the structure. It thus becomes a resonance level of the structure, similar to Friedel's virtual state in alloy theory, or resonance levels in quantum mechanical potential wells surrounded by potential barriers of finite width. If the soliton may decay by emitting radiation, it follows that it may also be excited by an incoming electromagnetic wave. The transmission resonance at point (4) of Fig. 3 is thus viewed as a consequence of resonant excitation of a soliton by the incoming wave. At one particular incoming field strength, the incoming wave matches into the soliton perfectly, the amplitude of the reflected wave is zero, and all the ener-

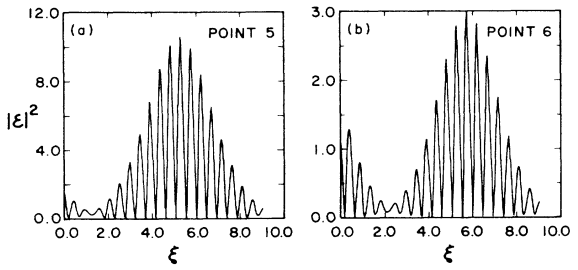

FIG. 6. The same as Fig. 4, but now the field intensity is calculated (a) at point 5, and (b) at point 6 of Fig. 3.

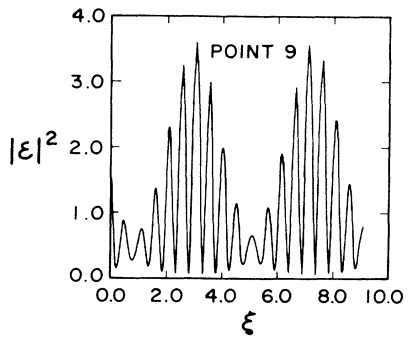

FIG. 8. The same as Fig. 4, but now the field is calculated at (a) point 9 of Fig. 3.

gy flows out the backside of the finite superlattice.

As we continue to progress to point 6 and point 7 of the transmissivity curve of Fig. 3, we see the second solitonlike structure progressively move into the superlattice from the left. At point 8, where we again realize a transmission resonance, we see resonant excitation of a soliton pair by the incident field. Note that the maximum field strength at point 8 is larger than that of either point 7 of point 9, so the two-soliton state is indeed a resonance of the superlattice structure.

As we move to point 9, we see a third soliton moving in from the left, while the remaining two compress and provide room for the new entity. There will be a third transmission resonance, we assume, though we have not carried our calculations further.

It remains for us to discuss how a physical system will behave in practice, when it is described by the transmissivity curve displayed in Fig. 3. To see this best, the information should be rearranged a bit. The abscissa in Fig. 3 is, to within a multiplicative constant, the input power. The quantity $|T|^2E_0^2$ is the output power, so a graph of the output of the superlattice, as a function of its input, proves useful in deducing the behavior of such a structure in practice. This is done in Fig. 9, where the information in Fig. 3 is rearranged into an input-output plot. In the theory of nonlinear devices, portions of the input-output curve with negative slope are unstable; thus, the segments of the curve from B to A, and E to D are unstable.

If we illuminate the system at very low power, the transmissivity is very small, as given by linear theory. As power is increased, we will move out along the horizontal axis from the origin to point A. A further increase in power will cause the system to switch to a new stable state. There are two possibilities, on either segment BC or onto segment EF. We know of no simple criterion for deciding which state the system will choose. If the calculation were continued to higher powers, segments ED and BC merge, to form a hairpin that is a mirror image of, say FED. Thus, if the system locks onto an operating point on BC upon increasing power beyond point A, when it reaches the end of the hairpin, a further increase will induce a transition to the extension of curve EF. Consider decreasing powers, and suppose the system is on curve EF. The operating point will move down EF to point E, where the superlattice has perfect transparency ($|T|^2=1$). A further decrease in power will cause it to jump down to curve BC, where, according to Fig. 3, $|T|^2\simeq 0.3$. Then continued decreases of power will move the operating point to B, where again $|T|^2\equiv 1$. Decreasing the power further will induce a transition to the point where the transmissivity is exponentially small. Thus, by choosing the operating point suitably, decreasing power can switch the system from a state where it is perfectly transmitting, to a state where the reflectivity is very close to unity.

The above calculations are for a finite superlattice, with twenty unit cells, each of which consists of a pair of films. As the length of the finite superlattice is de-

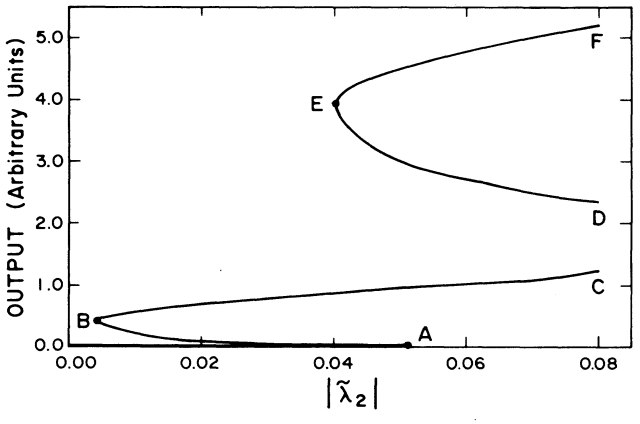

FIG. 9. The information in Fig. 3 is replotted, to provide the input-output relation of the superlattice. Recall $|\tilde{\lambda}_2|$ is proportional to E_0^2, and thus the incident power, and this is plotted as a function of $|T|^2E_0^2$, the intensity of the output beam. The transmissivity is unity at point B, and point E.

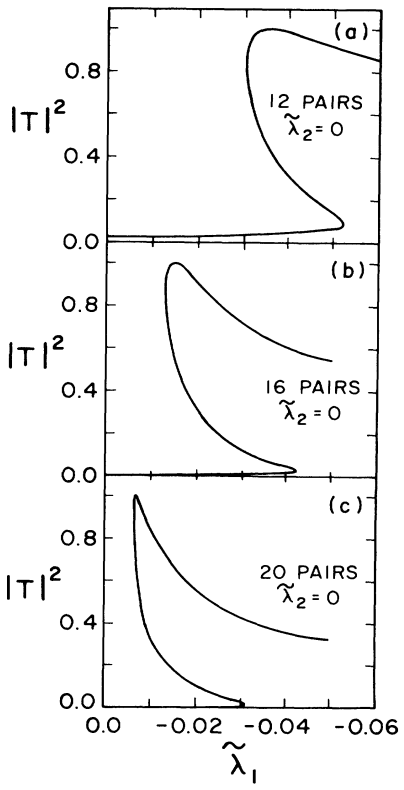

FIG. 10. For a set of finite superlattices each with a different number of unit cells (film pairs), we show the behavior of $|T|^2$ near the first resonance. We have, for the indices of refraction, $n_1=2.0$ and $n_1=1.5$, and we have chosen $\tilde{\lambda}_2=0$. The superlattices are illuminated with radiation in the stop gap analogous to that shown in Fig. 2, with frequency just above the bottom gap edge. The film thicknesses are $d_1=0.23\lambda_0/n_1$ and $d_2=0.23\lambda_0/n_2$, with λ_0 the vacuum wave length of the radiation. In (a), the superlattice has twelve unit cells, it has sixteen in (b), and twenty in (c).

creased, the power threshold for the onset of multivalued character in the transmission coefficient increases. We show this in Fig. 10, where for a finite superlattice with 12, 16, and 20 unit cells, we display the behavior of the transmissivity as a function of power, in the vicinity of the first nonlinear resonance.

It follows that as the superlattice is lengthened, the threshold drops. In practice, absorption is present, and on physical grounds it is clear that this will limit the length of the superlattice structures that will exhibit the behavior studied here. It is a nontrivial extension of the present analysis to incorporate absorption, unfortunately.

In this paper, we have shown how our earlier method for the study of the nonlinear optical response of a film may be extended to the case of a multilayer structure, with optically nonlinear films as constituents. The calculations we have carried out show how dielectric bilayers may be used as nonreciprocal elements, in regard to their bistability, and we find also that finite superlattices display soliton mediated optical switching, when illuminated by radiation in a stop gap.

ACKNOWLEDGMENTS

This research was supported by the U.S. Army Research Office (Durham, NC), through Grant No. PO426620.

---

[1]For a review, see A. A. Maradudin, *Proceedings of the Second International School of Condensed Matter Physics, Bulgaria, 1981* (World Scientific, New York, 1982).

[2]A recent paper, with a number of references to the literature, is K. M. Leung, Phys. Rev. B **32**, 5093 (1985).

[3]Wei Chen and D. L. Mills, Phys. Rev. B **35**, 524 (1987).

[4]D. L. Mills and S. E. Trullinger, Phys. Rev. B **36**, 947 (1987).

[5]Wei Chen and D. L. Mills, Phys. Rev. Lett. **58**, 160 (1987).

[6]François Delyon, Yves-Emmanuel Lévy, and Bernard Souillard, Phys. Rev. Lett. **57**, 2010 (1986).

[7]See the discussion that begins on p. 191 of C. Kittel, *Introduction to Solid State Physics* (Wiley, New York, 1976).

[8]We have recently completed a new series of calculations, based on the finite difference approach of Ref. 6. It seems possible, using this method, to study the soliton structures for frequencies within the gap, without encountering numerical difficulties. These calculations will be reported elsewhere. L. Kahn, N. S. Almeida, and D. L. Mills (unpublished).